



Fluorescence and visual immunoassay of HIV-1 p24 antigen in clinical samples via multiple selective recognitions of CdTe QDs

Zhuoyun Tang¹ · Zeliang Wei¹ · Ke Huang² · Yin hao Wei¹ · Dongdong Li¹ · Shixin Yan¹ · Jin Huang¹ · Jia Geng¹ · Chuanmin Tao¹ · Piaopiao Chen¹ · Binwu Ying¹

Received: 24 August 2021 / Accepted: 19 October 2021 / Published online: 17 November 2021
© The Author(s), under exclusive licence to Springer-Verlag GmbH Austria, part of Springer Nature 2021

Abstract

Human immunodeficiency virus (HIV) infection inflicts significant economic and social burdens on many countries worldwide. Given the substantial morbidity and mortality from HIV infection, there is an urgent need for accurate and early detection of the virus. In this study, immunofluorescence and visual techniques are described that detect the HIV-1 p24 antigen, which relied on selective recognition of Ag⁺/Ag nanoparticles (Ag NPs) and Cu²⁺/Cu⁺ using cadmium telluride quantum dots (CdTe QDs). After the sandwich immunoreactions were accomplished, the alkaline phosphatase (ALP) hydrolyzed L-ascorbic acid 2-phosphate (AAP) to form ascorbic acid (AA) that further reduces Ag⁺ and Cu²⁺ to Ag NPs and Cu⁺, respectively. This method was highly sensitive and selective and could detect as low as 1 pg/mL of p24 antigen by naked eyes and had a good linearity in the concentration range 1–100 pg/mL. When using Ag⁺ and Cu²⁺ as media, the limit of detection (LOD) of the new method was 0.3 pg/mL and 0.2 pg/mL, respectively. Compared with clinical electrochemiluminescence immunoassay (ECLIA) results and clinical data, this method demonstrated good consistency for the quantification of HIV-1 p24 antigen in 34 clinical serum samples. In addition, this method could accurately distinguish HIV from other viruses and infections such as *hepatitis B virus*, *systemic lupus erythematosus*, *hepatitis C virus*, *Epstein-Barr virus*, *cytomegalovirus*, *lipemia*, and *hemolysis*. Therefore, our dual-mode analysis method may provide additional solutions to identify clinical HIV infection.

Keywords Immunofluorescence · Visual detection · HIV-1 p24 antigen · Clinical samples · Selective recognition of CdTe QDs · Silver nanoparticles

Introduction

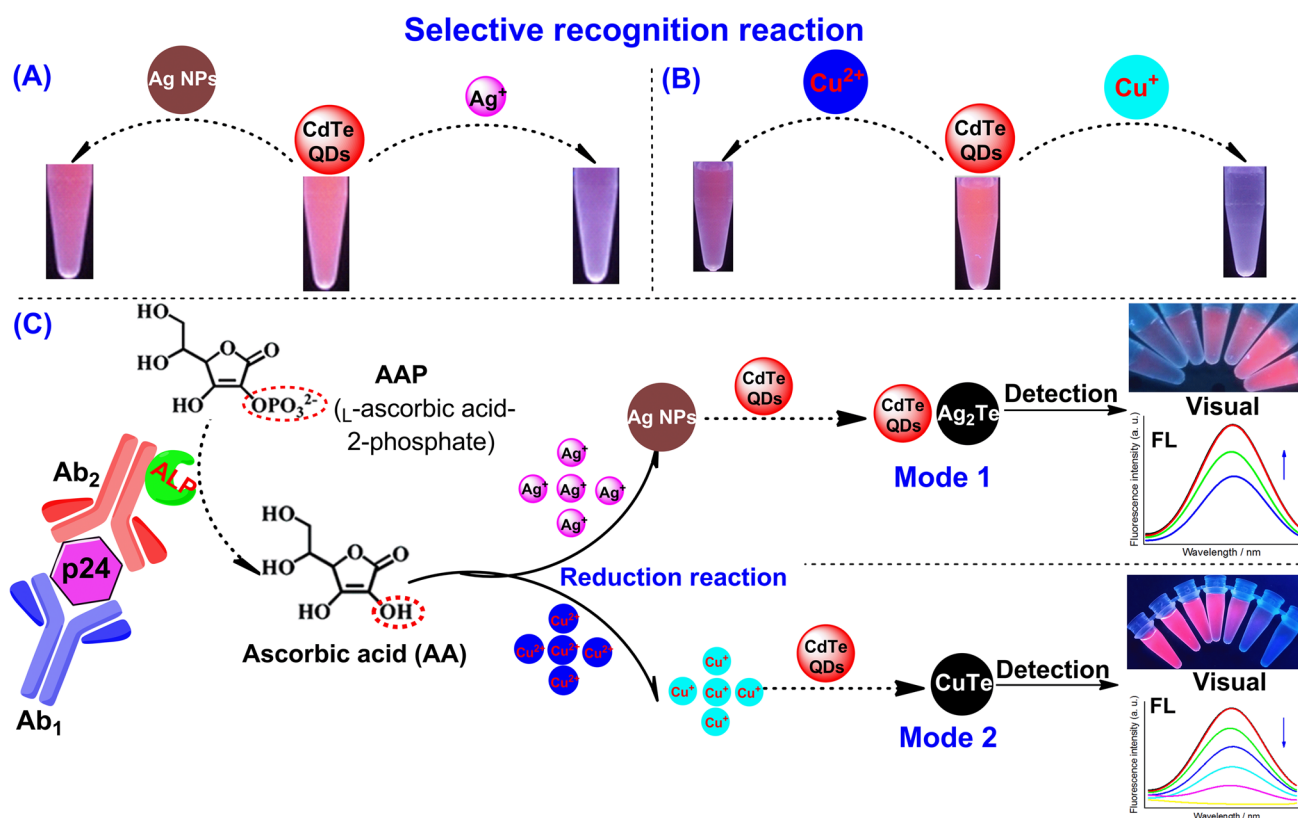
HIV infection/acquired immune deficiency syndrome is one of the major diseases causing significant morbidity and mortality worldwide. Effective management of HIV infection relies on early and accurate detection of the disease [1, 2]. The current HIV diagnosis techniques mainly detect the virus antigen and nucleic acid. Electrochemiluminescence immunoassay (ECLIA) is a highly sensitive and specific technique for quantitative detection of the HIV-1 p24 antigen and corresponding antibodies in human serum or plasma [3]. Despite its sensitivity of pg/mL, the technique is relatively expensive. The urgent need for rapid HIV diagnosis has accelerated the development of several HIV detection techniques, which include visual, colorimetric, fluorescence, photoelectrochemical, ECL, and electrochemical [4–11]. These methods offer unique and varied advantages in HIV diagnosis such as point-of-care testing (POCT) among others.

Zhuoyun Tang and Zeliang Wei Contributed equally to this work

- ✉ Jia Geng
geng.jia@scu.edu.cn
- ✉ Chuanmin Tao
taocm@scu.edu.cn
- ✉ Piaopiao Chen
chenpp0828@scu.edu.cn
- ✉ Binwu Ying
yingbinwu@scu.edu.cn

¹ Department of Laboratory Medicine, Department of Dermatology, State Key Laboratory of Biotherapy and Cancer Center, Med+X Center for Manufacturing, Laboratory of Ethnopharmacology, West China Hospital, Sichuan University, Chengdu 610041, Sichuan, China

² College of Chemistry and Material Science, Sichuan Normal University, Chengdu 610068, Sichuan, China



Scheme 1 Detection of HIV-1 p24 antigen based on immunoassay and selective recognition reaction. **A**, **B** Selective recognition reaction of QDs with Ag^+ /Ag NPs and Cu^{2+} / Cu^+ . **C** Immunofluorescence

and visualization detection of HIV-1 p24 antigen based on multiple selective recognitions of CdTe QDs

For POCT analysis, the choice of the signal readouts is extremely important. Various luminescent nanomaterials including QDs [12, 13], copper nanoclusters [14], copper nano-assemblies [15], silver nanoclusters [16], and gold nanoclusters [17, 18] are being applied in disease diagnosis and biological imaging among other functions. Among the luminescent nanomaterials, QDs offer significant advantages such as simple and rapid synthesis and low cost, require non-complicated or inexpensive devices, and have a long shelf life. Certain QDs (CdTe/CdSe QDs, etc.) have unique properties such as cation exchange with metal ions (Ag^+ / Hg^{2+} / Cu^{2+}). Cation exchange reaction (CER) readily and rapidly occurs at room temperature (RT), and the color of the solution before and after the reaction can be distinguished with the naked eyes [19–21]. QDs can identify metal ions, accurately distinguish metal ions of different valences, and identify complexes of metal ions such as Cu^{2+} / Cu^+ , Ag^+ /Ag NPs, Ag^+ /C– Ag^+ -C, and Hg^{2+} /T– Hg^{2+} -T [19, 22–25]. The selective CER property of QDs has been applied in analysis of AA and ALP, as well as in the diagnosis of urinary stone diseases by measuring the level of oxalate in urine in our preliminary work.

We developed a highly sensitive visual and fluorescent immunoassay for HIV-1 p24 antigen by combining multiple QD-based selective recognition reactions. The application of this method for the clinical diagnosis of HIV was also assessed with Ag^+ and Cu^{2+} as signal media, respectively [19, 23]. In this work, ALP hydrolyzes its substrate, AAP to produce reductant AA that further reduced Ag^+ and Cu^{2+} to Ag NPs and Cu^+ . Ag^+ /Ag NPs and Cu^{2+} / Cu^+ could then be identified using QDs, respectively (Scheme 1). Preliminary findings demonstrated the high sensitivity of the technique, which was comparable to that of the ECL method. As low as 1 pg/mL of p24 antigen could be recognized by naked eyes. The p24 antigen contents of 13 clinical HIV-positive samples which had been detected by our method were consistent with that of clinical ECLIA and RT-PCR findings. The specificity of the technique using 14 samples from the patients with other diseases (*hepatitis B virus*, *Epstein-Barr virus*, *cytomegalovirus*, *hepatitis C virus*, *systemic lupus erythematosus*, *lipemia*, and *hemolysis*) and 7 healthy individuals was also satisfactory. Therefore, the novel fluorescence method is an alternative technique for accurate HIV infection diagnosis.

Experimental section

Reagents

All reagents used in this study were of analytical grade level and were used without further purification. The 96-well plates were purchased from Boruizhi Biotechnology Company (Chengdu, China). Purity CdCl_2 , KBH_4 , $\text{Na}_3\text{C}_6\text{H}_5\text{O}_7 \cdot 2\text{H}_2\text{O}$, NaNO_3 , $\text{Mg}(\text{NO}_3)_2$, HCl , and NaOH were purchased from Kelong Chemical Reagents (Chengdu, China). 3-(*N*-Morpholino) propanesulfonic acid (MOPS) was purchased from Solarbio Technology Co., Ltd (Beijing, China). Anti-HIV-1 p24 antibody (Ab_1), anti-HIV-1 p24 antibody (Biotin- Ab_2), and HIV-1 p24 protein were purchased from Abcam Company (Shanghai, China). Streptavidin-alkaline phosphatase (SA-ALP), bovine serum albumin (BSA), human serum albumin (HSA), thrombin, transferrin, and papain were purchased from Sigma Company (Shanghai, China). Tween-20 was obtained from Sangon Biotechnology Co., Ltd (Shanghai, China). Na_2TeO_3 , 3-mercaptopropionic acid (MPA), L -ascorbic acid-2-phosphate (AAP), AgNO_3 , and CuSO_4 were purchased from Aladdin Reagent Co., Ltd (Shanghai, China). The buffers include blocking buffer, 1% (w/v, g mL^{-1}) BSA in 10 mM pH 7.4 MOPS buffer; assay buffer, 10 mM MOPS buffer (100 mM NaNO_3 , 2.5 mM $\text{Mg}(\text{NO}_3)_2$) at pH 7.4; and washing buffer, 10 mM MOPS buffer (100 mM NaNO_3 , 2.5 mM $\text{Mg}(\text{NO}_3)_2$) at pH 7.4 supplemented with 0.05% (v/v) Tween-20. Purity deionized water (18.2 $\text{M}\Omega\text{-cm}$) was obtained from the Milli-Q water system (Chengdu Ultrapure Technology Co., Ltd., Chengdu, China). All stock solutions and reagents were stored in a refrigerator at 4 °C before use.

Synthesis of CdTe QDs

The CdTe QDs were synthesized as previously described [25–27]. Briefly, 52 μL of MPA was added into freshly prepared 50 mL solution containing 0.5 mmol CdCl_2 and 0.2 g trisodium citrate before adjusting the pH to 10.5 using NaOH . Na_2TeO_3 (0.1 mmol) and KBH_4 (50 mg) were added into the above mixture before refluxing the final solution for 1 h to obtain the CdTe QDs. The CdTe QDs were precipitated using *n*-propanol and centrifuged at 11,000 rpm to obtain pure CdTe QDs. The red CdTe QDs were re-dispersed in high purity water before use.

Immunoassay

The process was performed using a 96-well plate. Briefly, 10 μL of 20 $\mu\text{g mL}^{-1}$ Ab_1 and 30 μL assay buffer were added in each well and incubated overnight at 4 °C. The

plate was washed three times using 200 μL of washing buffer to remove unbound antibodies. Uncoated active sites were saturated using 100 μL of blocking buffer at 37 °C for 1 h.

Forty microliters of HIV-1 p24 protein or serum samples with 60 μL assay buffer were added in the wells and incubated for 1 h at 37 °C. The wells were rinsed three times before adding 40 μL biotin- Ab_2 (5 $\mu\text{g mL}^{-1}$) and 60 μL assay buffer. The wells were rinsed three times after incubation for 1 h at 37 °C. To form the Ab_1 -p24- Ab_2 -SA-ALP sandwich complexes, 40 μL SA-ALP (5 $\mu\text{g mL}^{-1}$) and 60 μL assay buffer were added in the plate wells and incubated at RT for 15 min.

Fifty microliters of AAP (1 mM) and 100 μL assay buffer were added to the wells and incubated at 37 °C for 20 min before transferring the solution into EP tubes. CER was performed using either AgNO_3 or CuSO_4 .

CER was performed as follows: For AgNO_3 , 50 μL AgNO_3 (5 μM) was added into the tubes and incubated for 20 min at RT. After adding 0.5 μL CdTe QDs, a further 10 min incubation at RT was performed. For CuSO_4 , 5 μL CuSO_4 (50 μM) was added into the tubes and incubated at RT for 2.5 min. Then, 0.3 μL CdTe QDs was added and incubated 5 min at RT. Fluorescence was detected with 365 nm as excitation wavelength.

Results and discussion

Principles and feasibility of HIV-1 p24 antigen analysis

The dual-mode fluorescence and visual of HIV-1 p24 antigen analysis strategy are mainly based on immune reaction to form Ab_1 -p24- Ab_2 -SA-ALP sandwich complexes. The p24 antigen content positively correlated with ALP content. ALP catalyzes the production of reducing AA from AAP. AA reduces Ag^+ to Ag NPs or Cu^{2+} to Cu^+ . QDs selectively react with Ag^+ and Ag NPs (Scheme 1A, the quenching power of Ag^+ on QDs is stronger than that of Ag NPs, mode 1) and Cu^{2+} and Cu^+ (Scheme 1B, the quenching power of Cu^+ on QDs is stronger than that of Cu^{2+} , mode 2). P24 antigen is then detected based on the fluorescence signals (Scheme 1C). Herein, Ag^+ was used in the turn-on mode, whereas Cu^{2+} was used in the turn-off mode in the p24 antigen analysis strategy.

In our previous work, we found that QDs can selectively detect Ag^+ and Ag NPs and Cu^{2+} and Cu^+ [19, 23]. In this study, transmission electron microscopy (TEM) analysis of QDs under different conditions further validated these findings (Fig. 1). When Ag^+ was added to QDs (Fig. 1A), spherical QDs reunited to Ag_2Te significantly (Fig. 1B). Energy dispersive spectroscopy (EDS) (Fig. 1C and D) revealed that Ag could be found after CER. This implies that ion exchange occurred between Ag^+ and Cd^{2+} ,

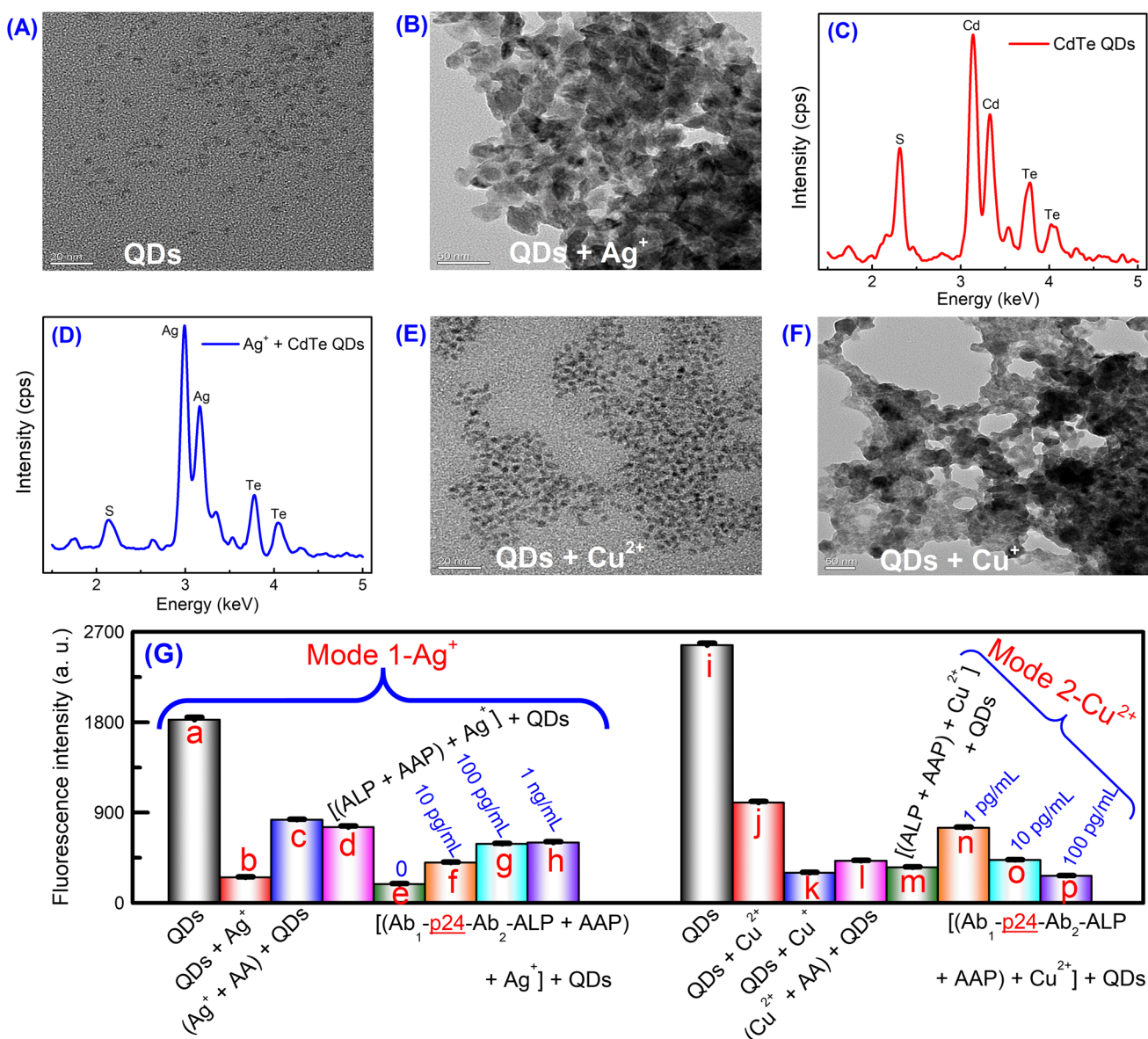


Fig. 1 Verification of the feasibility of selective recognition reaction and p24 antigen analysis. TEM images of QDs (**A**), QDs + Ag⁺ (**B**), QDs + Cu²⁺ (**E**), and QDs + Cu⁺ (**F**). The EDS images of CdTe QDs

(**C**) and Ag⁺ + CdTe QDs (**D**). **G** Feasibility. The error bars originated from at least three repeated tests

resulting in the formation of Ag₂Te. Both Cu²⁺ and Cu⁺ can trigger the CER resulting agglomeration of QDs to form CuTe. The agglomeration power of Cu⁺ on QDs was superior to that of Cu²⁺ (Fig. 1E vs. 1F) but comparable to that of Ag⁺. Fluorescence experiments further verified the above phenomenon in the absence of immune reaction (Fig. 1G). Ag⁺, Cu²⁺, and Cu⁺ significantly reduced the fluorescence signal of QDs. AA inhibits the quenching of QDs by Ag⁺ (Fig. 1G-b vs. 1G-c). The fluorescence quenching ability of Cu⁺ to QDs is superior to that of Cu²⁺ (Fig. 1G-j vs. 1G-k, l, and m). Furthermore, AA produced by hydrolyzation of AAP by ALP inhibited the quenching

of QDs by Ag⁺ with similar efficiency as directly added AA (Fig. 1G-c vs. 1G-d).

Regarding the feasibility of p24 immunoassay using Ag⁺ and Cu²⁺, the concentration of p24 antigen (0, 10 pg/mL, 100 pg/mL, and 1 ng/mL) was directly proportional to the intensity of the fluorescence signals. Therefore, Ag⁺ can potentially be used for p24 antigen analysis (Fig. 1G-e, f, g, and h). Different from Ag⁺, when using Cu²⁺, the fluorescence signal of the solution decreased (Fig. 1G-n, o, p) with an increase in p24 antigen concentration of (1–100 pg/mL). This resulted from the generation of Cu⁺. Therefore, Cu²⁺ is also efficient for p24 antigen analysis, and its sensitivity is similar to that of Ag⁺.

Analytical performance of HIV-1 p24 antigen

Under the optimized conditions (Figs. S1 and S2), analytical performance of p24 antigen using Ag⁺ as a medium was investigated. Different p24 concentrations generated varied color intensities under UV light irradiation, visible to the naked eye. For instance, the emission generated by 1 pg/mL p24 antigen was significantly stronger than 0.1 pg/mL p24

(Fig. 2A). Between 1 and 100 pg/mL, the red color of the solutions deepened with increase in p24 concentration. We found a perfect linear relationship between the intensity of the fluorescence signals and the logarithm of p24 concentration (1–100 pg/mL) (Fig. 2B and C). The linear equation of the relationship can be expressed as $Y = 163\text{Log}C + 135$ ($R^2 = 0.996$). The LOD of this method was 0.3 pg/mL (3 S/N, n = 11). The LOD was calculated without p24 antigen given that the fluorescence signal was three standard

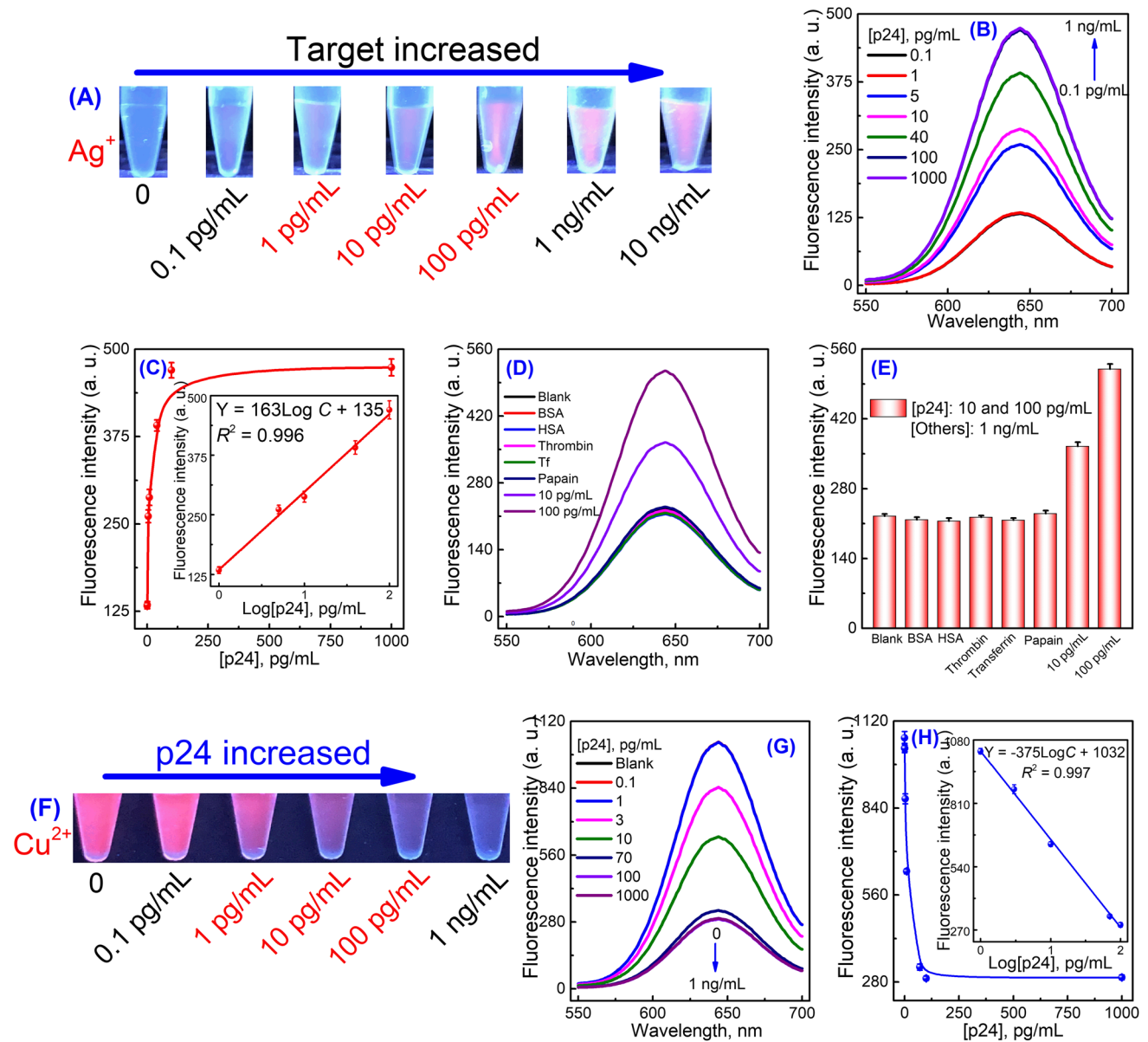


Fig. 2 Analytical performance and selectivity of p24 antigen via multiple selective CER. Mode 1 (Ag⁺-mediated recognition): **A** Color change caused by adding increasing concentration of p24 antigen, **B, C** fluorescence intensity change caused the addition of different concentration of p24 antigen, and **D, E** fluorescence intensity change caused by adding different types and concentrations of inter-

fering proteins. Mode 2 (Cu²⁺-mediated recognition): **F** Color change caused by adding increasing concentration of p24 antigen and **G, H** Fluorescence intensity change caused by the addition of different concentration of p24 antigen. The error bars originated from at least three repeated tests

deviations higher than the background signals [28, 29] and comparable to most existing analytical methods (Table 1). Although the sensitivity of this strategy is not optimal, the advantages such as simple to use at room temperature, without instruments, and uses low-cost reagents with visual analysis make it stand out. The reproducibility of this method was assessed using 10 pg/mL of HIV-1 p24 antigen. The relative standard deviation (RSD) of five consecutive detections was 3.6%. The specificity of the method was assessed using proteins potentially present in clinical samples for HIV-1 diagnosis. P24 antigen (10 and 100 pg/mL) induced significantly stronger fluorescence, relative to other interference proteins used at higher concentrations (1 ng/mL, Fig. 2D and E).

When using Cu^{2+} for p24 antigen detection, in contrast with Ag^+ , the color of the solution weakened gradually with increase in p24 concentration 1–100 pg/mL (Fig. 2F). The sensitivity using Cu^{2+} was similar to that of Ag^+ , with the lower limit of visual reading of 1 pg/mL. The fluorescence intensity of the solutions and the logarithm of p24 concentration (1–100 pg/mL) also displayed a good linear relationship (Fig. 2G and H). The LOD when using Cu^{2+} was 0.2 pg/mL, similar to that of Ag^+ . This method was reproducible, and the RSD of five consecutive detections of 10 pg/mL HIV-1 p24 antigen was 4.2%.

In summary, the p24 antigen analysis system based on immune recognition and visual/fluorescent changes of QDs caused by Ag^+ or Cu^{2+} is highly sensitive and selective. In contrast, the Ag^+ -assisted mode is more stable, but the medium should avoid halogen elements. The Cu^{2+} -assisted

mode analysis is fast and requires high levels of operators. The method we presented is a proof-of-concept study. With the automatic reaction and instrumentations applied in commercial or clinical applications, future low-cost, high sensitivity, and integrated detection machines could be applied in this study.

Application of this strategy in clinical samples

The core of an analysis method is its practical application. We compared the utility of this method with that of ECLIA methods using 34 clinical samples, including 13 HIV-positive samples (different ages, gender, and different periods), 14 samples from patients with other diseases, and 7 healthy individuals. The accuracy of our method (mode 1, Fig. 3A) was comparable to that of the ECLIA method (Roche, COI, Fig. 3B), where the linear correlation coefficient was as high as 0.996 (Fig. 3C). The performance of our test was also consistent with that of PCR findings (Fiebig stage and RNA results of PCR analysis, Table S1) [34]. Analysis of samples from patients with *hepatitis B virus*, *hepatitis C virus*, *Epstein-Barr virus*, *cytomegalovirus*, *systemic lupus erythematosus*, lipemia, and hemolysis demonstrated that the method was highly specific (Fig. 3D). The specificity of the method was further validated using 7 samples from healthy individuals (Table S1, Fig. 3D). Overall, the system is highly sensitive and specific for p24 antigen detection in clinical

Table 1 Comparison of immune methods for the determination of HIV p24 antigen

Method	System	Linear range; LOD	Verify practicality	Reference
Naked eye	Gold nanoparticles	NM ^g ; 10 ⁻¹⁸ g/mL	HIV-infected serum	[5]
Visual	Microfluidic, multicolor immunosensor	0–3 ng/mL; 0.5 ng/mL	Serum; recovery	[9]
Visual	Centrifugal microchannel array chip, TMB	NM; 110 pg/mL	HIV-positive serum	[30]
FL ^a	Peptidic β -sheets; Congo red	0.1–150 pg/mL; 0.61 pg/mL	HIV-positive serum	[4]
FL	Gold nanoclusters	5–1000 pg/mL; 5 pg/mL	HIV-positive serum samples	[8]
FL	Ce(III) coordination polymer	4–28 pg/mL; 1.1 pg/mL	Healthy human serum; recovery	[6]
FL	o-Phenylenediamine, HRP	1.4–90 pg/mL; 0.5 pg/mL	Commercial human serum; recovery	[31]
PEC ^b	Liposome-amplified	1.0 pg/mL–50 ng/mL; 0.63 pg/mL	Artificially positive human serum; recovery	[11]
ECL ^c	P-RGO@Au@Ru-SiO ₂ composite	1 pg/mL–1 ng/mL; 1 pg/mL	Human serum; recovery	[10]
EC ^d	Graphene oxide-HRP-thionine	0.5 pg/mL–8.5 ng/mL; 0.15 pg/mL	Human serum	[7]
EC	Fe ₃ O ₄ @SiO ₂ nanomagnetic probes	0.001–10 ng/mL; 0.5 pg/mL	Human serum; recovery	[32]
CL ^e	Microfluidic, PEO-PPO-PEO ^f	0.86–800 pg/mL; 0.86 pg/mL	HIV-positive serum	[33]
FL/visual	QDs; Ag ⁺ ; Cu ²⁺ ; ALP	1–100 pg/mL; 0.25 pg/mL	Serum from patients with HIV positive	This work

^aFluorescence; ^bphotoelectrochemical; ^celectrochemiluminescence; ^delectrochemical; ^echemiluminescence; ^fpoly(ethylene oxide)-poly(propylene oxide) triblock copolymer; ^gnot mentioned

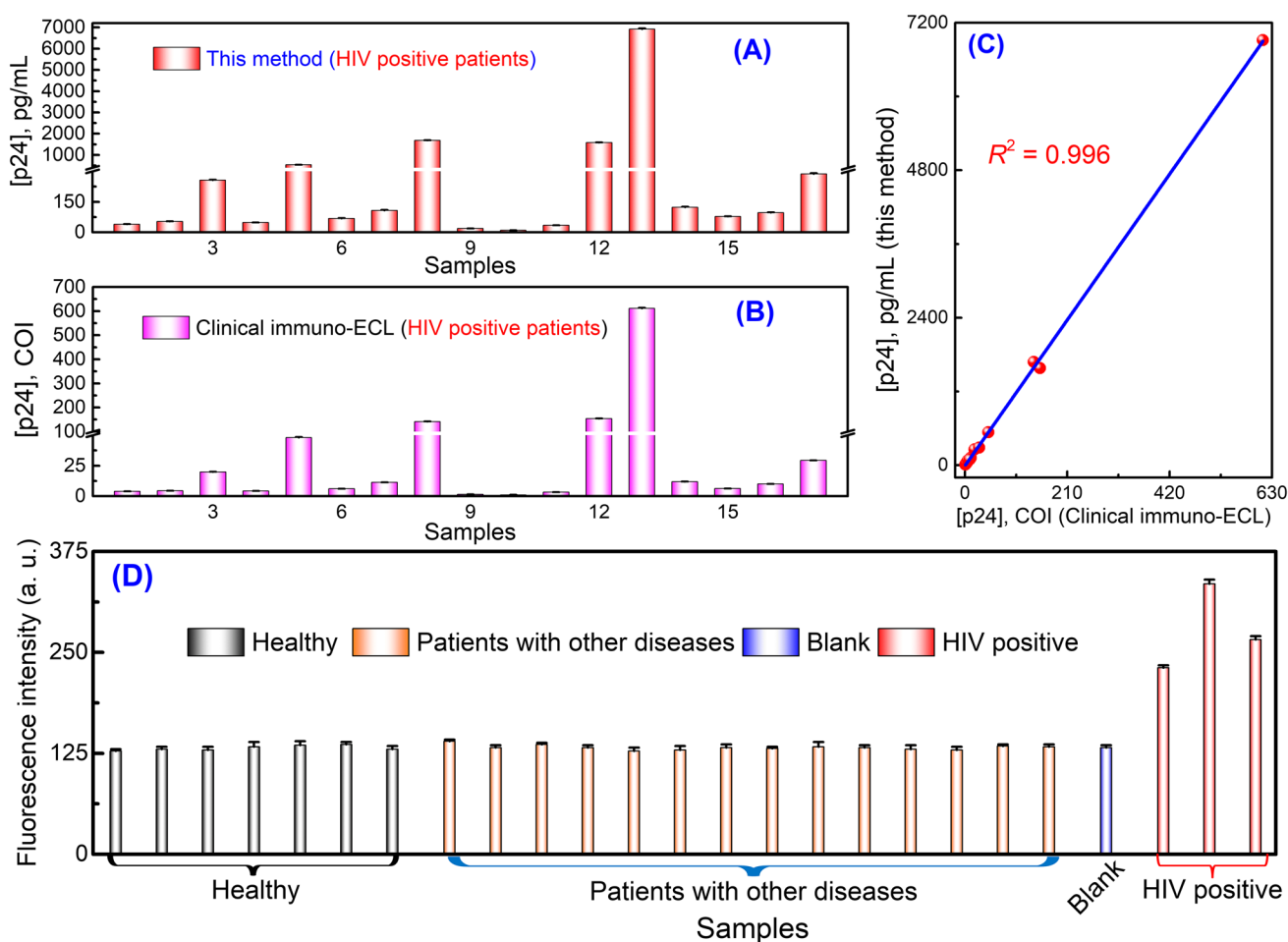


Fig. 3 Analysis results of clinical serum samples. The concentration of p24 antigen in HIV-positive patients' serums detected by our method (A) and clinical immuno-ECL strategy (B). C Consistency of clinical ECL and our method on HIV-positive samples. D Anti-inter-

ference ability of the method was evaluated by using serum samples from patients with different diseases and healthy persons. The error bars resulted from at least three repeated measurements

serum samples. It is therefore a feasible alternative for HIV infection diagnosis.

Conclusions

We successfully developed a highly sensitive and specific immunofluorescence and visual method for HIV diagnosis by detecting the p24 antigen. The method relied on selective detection of Ag^+/Ag NPs and $\text{Cu}^{2+}/\text{Cu}^+$ using QDs. The method is relatively economic, with a LOD of pg/mL level, visible to the naked eyes. The performance of this method for HIV infection diagnosis from clinical samples was comparable to the traditional ECLIA and PCR techniques. Given the superior luminescence, the stability of QDs, and the portability of the fluorometer, this new method offers a strong alternative for HIV diagnosis. Given the analytical sensitivity of this strategy for p24 antigen, if combining with

nucleic acid signal amplification strategies, it will be promising to achieve ultra-early HIV infection screening [35–39]. In addition, the color recognition POCT mode has certain limitations for color blind or color weak people, which can be improved by changing the reading mode, such as distance or height.

Supplementary Information The online version contains supplementary material available at <https://doi.org/10.1007/s00604-021-05075-7>.

Acknowledgements We would like to thank Dr. Shanling Wang of the Analytical & Testing Center of Sichuan University for TEM work.

Author contributions Piaopiao Chen, Zhuoyun Tang and Zeliang Wei: performed the experiments and wrote the manuscript; Piaopiao Chen, Jia Geng, Chuanmin Tao and Binwu Ying: designed the experiments and revised the manuscript;

Ke Huang and Shixin Yan: performed the synthesis and characterization of QDs and data processing;

Yinhao Wei, Dongdong Li and Jin Huang: afford provided the clinical samples and performed clinical experiments.

Funding This work was supported by the Science and Technology Planning Project of Sichuan (2020YFS0136); National Natural Science Foundation Regional Innovation and Development (U20A20394); Sichuan Science and Technology Program (2021YFS0232); Sichuan Province Health and Family Planning Commission (Sichuan Health Office issued [2017] 70); Science and Technology Project of Chengdu (2017-CY02-00018-GX); China Postdoctoral Science Foundation (2019M653391); Sichuan University Post-Doctor Research Project (2020SCU12051); and Post-Doctor Research Project, West China Hospital, Sichuan University (2020HXBH065).

Declarations

Conflict of interest The authors declare no competing interests.

References

- Cornett JK, Kirn TJ (2013) Laboratory diagnosis of HIV in adults: a review of current methods. *Clin Infect Dis* 57:712–718
- Tominski D, Katchanov J, Driesch D, Daley MB, Liedtke A, Schneider A, Slevogt H, Arasteh K, Stocker H (2017) The late-presenting HIV-infected patient 30 years after the introduction of HIV testing: spectrum of opportunistic diseases and missed opportunities for early diagnosis. *HIV Med* 18:125–132
- Zhang SY, Garcia-D'Angeli A, Brennan JP, Huo Q (2014) Predicting detection limits of enzyme-linked immunosorbent assay (ELISA) and bioanalytical techniques in general. *Analyst* 139:439–445
- Cao HY, Liu Y, Sun HY, Li ZL, Gao Y, Deng XL, Shao YM, Cong YL, Jiang XY (2020) Increasing the assembly efficacy of peptidic beta-sheets for a highly-sensitive HIV detection. *Anal Chem* 92:11089–11094
- De La Rica R, Stevens MM (2012) Plasmonic ELISA for the ultrasensitive detection of disease biomarkers with the naked eye. *Nat Nanotechnol* 7:821–824
- Du MY, Li NX, Mao GB, Liu YC, Wang XX, Tian SB, Hu QX, Ji XH, Liu YL, He ZK (2019) Self-assembled fluorescent Ce(III) coordination polymer as ratiometric probe for HIV antigen detection. *Anal Chim Acta* 1084:116–122
- Fang YS, Huang XJ, Wang LS, Wang JF (2015) An enhanced sensitive electrochemical immunosensor based on efficient encapsulation of enzyme in silica matrix for the detection of human immunodeficiency virus p24. *Biosens Bioelectron* 64:324–332
- Kurdekar AD, Chunduri LA, Manohar CS, Haleyrigirisetty MK, Hewlett IK, Venkataramaniah K (2018) Streptavidin-conjugated gold nanoclusters as ultrasensitive fluorescent sensors for early diagnosis of HIV infection. *Sci Adv* 4:eaar6280.
- Liu D, Zhang YQ, Zhu MY, Yu ZZ, Ma XM, Song YL, Zhou SF, Yang CY (2020) A microfluidic-integrated multicolor immunosensor for visual detection of HIV-1 p24 antigen with the naked eyes. *Anal Chem* 92:11826–11833
- Zhou LM, Huang JS, Yu B, Liu Y, You TY (2015) A novel electrochemiluminescence immunosensor for the analysis of HIV-1 p24 antigen based on P-RGO@Au@Ru-SiO₂ composite. *ACS Appl Mater Interfaces* 7:24438–24445
- Zhuang JY, Han B, Liu WC, Zhou JF, Liu KW, Yang DP, Tang DP (2018) Liposome-amplified photoelectrochemical immunoassay for highly sensitive monitoring of disease biomarkers based on a split-type strategy. *Biosens Bioelectron* 99:230–236
- Liu SY, Yan AM, Guo WYZ, Fang YY, Dong QJ, Li RR, Ni SN, Sun Y, Yang WC, Yang GF (2020) Human neutrophil elastase activated fluorescent probe for pulmonary diseases based on fluorescence resonance energy transfer using CdSe/ZnS quantum dots. *ACS Nano* 14:4244–4254
- Peckys DB, Quint C, de Jonge N (2020) Determining the efficiency of single molecule quantum dot labeling of HER2 in breast cancer cells. *Nano Lett* 20:7948–7955
- Ouyang XY, Wang MF, Guo LJ, Cui CJ, Liu T, Ren YA, Zhao Y, Ge ZL, Guo XN, Xie G, Li J, Fan CH, Wang LH (2020) DNA nanoribbon-templated self-assembly of ultrasmall fluorescent copper nanoclusters with enhanced luminescence. *Angew Chem Int Ed* 59:11836–11844
- Zhou TY, Zhu JY, Gong LS, Nong LT, Liu JB (2019) Amphiphilic block copolymer-guided in situ fabrication of stable and highly controlled luminescent copper nanoassemblies. *J Am Chem Soc* 141:2852–2856
- Wang S, Lu S, Zhao J, Yang X (2019) A ratiometric fluorescent DNA radar based on contrary response of DNA/silver nanoclusters and G-quadruplex/crystal violet. *ACS Appl Mater Interfaces* 11:25066–25073
- Goswami N, Lin FX, Liu YB, Leong DT, Xie JP (2016) Highly luminescent thiolated gold nanoclusters impregnated in nanogel. *Chem Mater* 28:4009–4016
- Zhao Y, Zhuang SL, Liao LW, Wang CM, Xia N, Gan ZB, Gu WM, Li J, Deng HT, Wu ZK (2020) A dual purpose strategy to endow gold nanoclusters with both catalysis activity and water solubility. *J Am Chem Soc* 142:973–977
- Chen PP, Bai YJ, Tang Y, Yan SX, Wang XY, Wei WR, Wang J, Zhang M, Ying BW, Geng J (2020) Rapid and highly sensitive visual detection of oxalate for metabolic assessment of urolithiasis *via* selective recognition reaction of CdTe quantum dots. *J Mater Chem B* 8:7677–7684
- Li JS, Zhang TR, Ge JP, Yin YD, Zhong WW (2009) Fluorescence signal amplification by cation exchange in ionic nanocrystals. *Angew Chem Int Ed* 48:1588–1591
- Son DH, Hughes SM, Yin YD, Alivisatos AP (2004) Cation exchange reactions in ionic nanocrystals. *Science* 306:1009–1012
- Chen PP, Huang K, Dai R, Sawyer E, Sun K, Ying BW, Wei XW, Geng J (2019) Sensitive CVG-AFS/ICP-MS label-free nucleic acid and protein assays based on a selective cation exchange reaction and simple filtration separation. *Analyst* 144:2797–2802
- Chen PP, Yan SX, Sawyer E, Ying BW, Wei XW, Wu ZZ, Geng J (2019) Rapid and simple detection of ascorbic acid and alkaline phosphatase *via* controlled generation of silver nanoparticles and selective recognition. *Analyst* 144:1147–1152
- Hu PY, Wang X, Wei L, Dai R, Yuan X, Huang K, Chen PP (2019) Selective recognition of CdTe QDs and strand displacement signal amplification-assisted label-free and homogeneous fluorescence assay of nucleic acid and protein. *J Mater Chem B* 7:4778–4783
- Chen PP, Wang Y, He YQ, Huang K, Wang X, Zhou RH, Liu TYH, Qu RL, Zhou J, Peng W, Li M, Bai YJ, Chen J, Huang J, Geng J, Xie Y, Hu W, Ying BW (2021) Homogeneous visual and fluorescence detection of circulating tumor cells in clinical samples *via* selective recognition reaction and enzyme-free amplification. *ACS Nano* 15:11634–11643
- Chen PP, Qu RL, Peng W, Wang X, Huang K, He YQ, Zhang XL, Meng YM, Liu TYH, Chen J, Xie Y, Huang J, Hu Q, Geng J, Ying BW (2021) Visual and dual-fluorescence homogeneous sensor for the detection of pyrophosphatase in clinical hyperthyroidism samples based on selective recognition of CdTe QDs and coordination polymerization of Ce³⁺. *J Mater Chem C* 9:4141–4149
- Wang X, Chen X, Zhou RH, Hu PY, Huang K, Chen PP (2021) Filter-assisted separation of multiple nanomaterials: mechanism and application in atomic/mass spectrometry/fluorescence label-free multimode bioassays. *Anal Chem* 93:3889–3897
- Chen PP, Yang P, Zhou RX, Yang X, Chen JB, Hou XD (2018) Selective reduction-based, highly sensitive and homogeneous

- detection of iodide and melamine using chemical vapour generation-atomic fluorescence spectrometry. *Chem Commun* 54:4696–4699
29. Ma W, Yin HH, Xu LG, Wu XL, Kuang H, Wang LB, Xu CL (2014) Ultrasensitive aptamer-based SERS detection of PSAs by heterogeneous satellite nanoassemblies. *Chem Commun* 50:9737–9740
30. Li FY, Zheng Y, Wu J, Zhao L, Shui LL, Pu QS, Liu SR (2019) Smartphone assisted immunodetection of HIV p24 antigen using reusable, centrifugal microchannel array chip. *Talanta* 203:83–89
31. Zhang Y, Yang H, Yu JP, Wei HP (2016) Rapid and sensitive detection of HIV-1 p24 antigen by immunomagnetic separation coupled with catalytic fluorescent immunoassay. *Anal Bioanal Chem* 408:6115–6121
32. Gan N, Du XW, Cao YT, Hu FT, Li TH, Jiang QL (2013) An ultrasensitive electrochemical immunosensor for HIV p24 based on Fe₃O₄@ SiO₂ nanomagnetic probes and nanogold colloid-labeled enzyme-antibody copolymer as signal tag. *Materials* 6:1255–1269
33. Li ZL, Liu Y, Chen XM, Cao HY, Shen HY, Mou L, Deng XL, Jiang XY, Cong YL (2020) Surface-modified mesoporous nanofibers for microfluidic immunosensor with an ultra-sensitivity and high signal-to-noise ratio. *Biosens. Bioelectron.* 166:112444.
34. Fiebig EW, Wright DJ, Rawal BD, Garrett PE, Schumacher RT, Peddada L, Heldebrant C, Smith R, Conrad A, Kleinman SH, Busch MP (2003) Dynamics of HIV viremia and antibody seroconversion in plasma donors: implications for diagnosis and staging of primary HIV infection. *AIDS* 17:1871–1879
35. Zhu LP, Chen DS, Lu XH, Qi Y, He P, Liu CH, Li ZP (2018) An ultrasensitive flow cytometric immunoassay based on bead surface-initiated template-free DNA extension. *Chem Sci* 9:6605–6613
36. Yamashige R, Kimoto M, Okumura R, Hirao I (2018) Visual detection of amplified DNA by polymerase chain reaction using a genetic alphabet expansion system. *J Am Chem Soc* 140:14038–14041
37. Liu M, Zhang Q, Kannan B, Botton GA, Yang J, Soleymani L, Brennan JD, Li YF (2018) Self-assembled functional DNA superstructures as high-density and versatile recognition elements for printed paper sensors. *Angew Chem Int Ed* 57:12440–12443
38. Xing C, Doi J, Huang YQ, Lin YH, Zhang KL, Lu CH, Yang HH (2019) Active self-assembly of train-shaped DNA nanostructures via catalytic hairpin assembly reactions. *Small* 15:1901795
39. Huang P-JJ, de Rochambeau D, Sleiman HF, Liu JW (2020) Target self-enhanced selectivity in metal-specific DNazymes. *Angew Chem Int Ed* 59:3573–3577

Publisher's note Springer Nature remains neutral with regard to jurisdictional claims in published maps and institutional affiliations.